

Article

Selective Oxidation of Methane over Fe-Zeolites by *In Situ* Generated H₂O₂

Jongkyu Kang¹ and Eun Duck Park^{1,2,*} 

¹ Department of Energy Systems Research, Ajou University, 206, World cup-ro, Yeongtong-Gu, Suwon-si 16499, Korea; jong458@ajou.ac.kr

² Department of Chemical Engineering, Ajou University, 206, World cup-ro, Yeongtong-Gu, Suwon-si 16499, Korea

* Correspondence: edpark@ajou.ac.kr

Received: 21 February 2020; Accepted: 3 March 2020; Published: 5 March 2020



Abstract: Liquid-phase selective oxidation of methane into methane oxygenates, including methanol and formic acid, with molecular oxygen was investigated using Fe-zeolites and Pd/activated carbon in the presence of molecular hydrogen as a reducing agent. Various Fe-zeolites such as Fe-ZSM-5, Fe-mordenite, Fe- β , Fe-Y, and Fe-ferrierite were prepared by ion-exchange and compared for this reaction. Among them, Fe-ZSM-5 was selected for further study because this catalyst showed high activity in the selective oxidation of methane with relatively less leaching. Further, the effect of reaction temperature, pH, and the amount of catalyst was examined, and detailed investigations revealed that the leached Fe species, which were facilitated in the presence of acid, were mainly responsible for methane oxidation under the given reaction conditions.

Keywords: partial oxidation of methane; liquid-phase oxidation; hydrogen peroxide; formic acid; methane oxygenates

1. Introduction

Methane, a major component of natural gas, is considered as a clean energy resource because it emits the lowest amount of CO₂ per unit of energy produced during combustion of hydrocarbons. Recent commercial production of shale gas has raised expectations for the wide utilization of methane as a chemical feedstock. Owing to its abundance and cleanliness, methane is expected to replace coal and oil in the energy and chemical sector until sustainable resources are economically viable [1]. Although methane has been utilized as a chemical feedstock via syn gas (a mixture of CO and H₂), this indirect process has been applied to only limited cases because it is an energy-intensive process. On the other hand, the direct conversion of methane is extremely onerous because its high C-H bond dissociation energy (439 kJ/mol) makes it difficult to selectively convert into value-added chemicals [2,3].

The partial oxidation of methane has been mainly investigated either in the gas phase at relatively high temperatures or in the liquid phase at low temperatures. The gas-phase partial oxidation of methane has been reported over metal ion-exchanged zeolites [4–6] using O₂ [7,8], N₂O [9,10], and H₂O [11,12]. The liquid-phase partial oxidation of methane has been demonstrated over several catalyst systems including Pt [13–16], Pd [17,18], Rh [19,20], Os [21], Hg [22], Cu [23], V [24], Fe [25,26], Eu [27], and Co [28,29] using different oxidants such as SO₃ [17,23], K₂S₂O₈ [30], and H₂O₂ [24–26]. In the case of liquid-phase systems, strong acids such as sulfuric acid and trifluoroacetic acid have been frequently used to convert methane into stable intermediates such as methyl bisulfate and methyl trifluoroacetate. However, the corrosive nature of the acids, and requirement of expensive oxidants and an excessive amount of water in the additional hydrolysis step for methanol synthesis from methanol derivatives, are problematic. Therefore, investigations into the partial oxidation of methane in the

aqueous phase are actively underway. Hutchings and co-workers have conducted methane oxidation over Au-Pd nanoparticle colloids by depositing them on TiO₂ or ZSM-5 [31,32]. Tsubaki et al. have also reported an Au-Pd catalyst supported on carbon materials to convert methane into methane oxygenates with *in situ* generated H₂O₂ [33]. Recently, Xiao et al. reported high methane conversions using a catalyst system in which the concentration of H₂O₂ in Au-Pd@zeolite could be enriched by surface modification [34].

In our previous study, we reported the aqueous-phase partial oxidation of methane using homogeneous Fe catalysts and Pd/C, where H₂O₂ was generated *in situ* from H₂ and O₂ [35]. In this study, Fe-zeolites were prepared via an ion-exchange method to immobilize the homogeneous Fe catalysts into the zeolite matrix, and were applied to the liquid-phase partial oxidation of methane.

2. Results

2.1. Catalyst Characterization

The metal content and Brunauer Emmett Teller (BET) surface area of the Fe-zeolites are listed in Table S1. It is noteworthy that the Fe content in each Fe-zeolite was different even though the same mother liquor with the same Fe concentration was used during catalyst preparation. The Fe content for each Fe-zeolite decreased in the following order: Fe-mordenite > Fe-β > Fe-ZSM-5 > Fe-Y >> Fe-ferrierite. The Fe content was not dependent on the Al content or Al/Si ratio. The BET surface area of each Fe-zeolite decreased slightly as compared with that of each zeolite itself. To identify the change in the bulk crystalline structure of each Fe-zeolite during its preparation, X-ray diffraction (XRD) patterns of the parent zeolites and Fe-zeolites were obtained and compared. There was no noticeable change in the XRD patterns (Figure S1), which implied that the bulk crystalline structure was well preserved and there was no bulk iron oxide in Fe-zeolites.

The UV-Vis spectra of the Fe-zeolites were obtained to probe each constituent Fe species. Figure 1 shows that a main peak appeared in the wavelength range of 250–300 nm for all Fe-zeolites and a shoulder peak could be observed at above 350 nm for some Fe-zeolites with high Fe content. It is generally accepted that each Fe species in the Fe-zeolite has its own characteristic peak in the UV-Vis spectra [36,37]: (a) Fe species with tetrahedral coordination (200–240 nm) such as framework Fe species in Fe-silicalite, (b) square-pyramidal and distorted octahedra such as isolated Fe ions on alumina surface (250–300 nm), (c) Fe³⁺ ions in small oligonuclear clusters (300–450 nm), and (d) bulk Fe oxide particles on zeolite (above 450 nm). Furthermore, the Fe species present in all Fe-zeolites are mainly isolated Fe ions located on an ion-exchangeable site in the zeolite. The presence of iron oligonuclear clusters was confirmed in Fe-mordenite, Fe-ZSM-5, and Fe-β, which have relatively high Fe contents compared to the other zeolites.

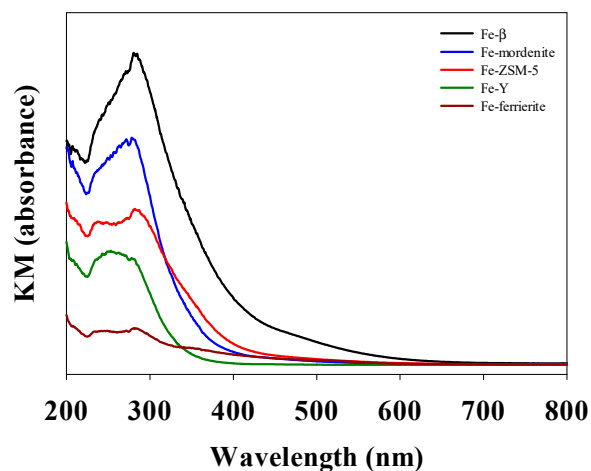


Figure 1. UV-Vis spectra of various Fe-zeolite catalysts prepared via an ion-exchange method.

2.2. Catalytic Performance

The liquid-phase partial oxidation of methane was carried out with Fe-zeolites and Pd/activated carbon (AC) as the catalyst in the presence of H₂ and O₂. The pH of the aqueous solution was controlled to 1.3 using H₂SO₄. As shown in Table 1, the catalytic performance was strongly dependent on the Fe-zeolite. Fe-Y and Fe-β showed much higher catalytic activity in terms of total product yield compared to the other Fe-zeolites. As each Fe-zeolite had different Fe content, the turnover number (TON) was also calculated (Table 1). The TON decreased in the following order: Fe-Y > Fe-β > Fe-ZSM-5 > Fe-mordenite > Fe-ferrierite. The selectivity to methane oxygenates generally decreased with increasing total product yield, which is reasonable because the partial oxidation of methane is a consecutive reaction from methane to CO₂ through methyl hydroperoxide, methanol, and formic acid [25]. Even though Fe-Y and Fe-β showed high catalytic activity, the inductively coupled plasma (ICP) analysis of the liquid remaining after the reaction revealed that large fractions of Fe and Al present in Fe-Y and Fe-β had leached out during the reaction (Table S2). This implied that these catalysts were unsuitable for the heterogenization of the homogeneous catalyst system. Considering both the catalytic performance and the stability, Fe-ZSM-5 was selected for a further study.

Table 1. Catalytic activity of various Fe-zeolites and 1 wt. % Pd/AC for partial oxidation of methane with H₂ and O₂. ^a

Fe Catalyst	[H ₂ O ₂] _{fin} (mM)	Product (μmol)				Total Product	Selectivity to Methane Oxygenates ^b (%)	TON ^c
		CH ₃ OH	HCOOH	CH ₃ OOH	CO ₂			
Fe-ZSM-5	9	22	52	0	16	90	82	11
Fe-mordenite	7	14	57	0	22	93	76	7.0
Fe-β	2	15	144	1	131	291	55	28
Fe-Y	7	10	139	5	167	321	48	51
Fe-ferrierite	4	5	4	0	0	9	100	4.6

^a Reaction conditions: 50 mg of Fe-zeolite in Table S1 and 50 mg of 1 wt. % Pd/AC; reaction temperature = 30 °C; reaction time = 30 min; V_{liquid} = 30 mL; [H₂SO₄] = 15 mM; V_{gas} = 90 mL; P_{CH₄} = 15 bar; P_{H₂} = 3 bar; P_{Air} = 10 bar.

^b Selectivity to methane oxygenates was calculated as [moles of products excluding CO₂]/[moles of total products] × 100 (%). ^c Turnover number (TON) was calculated as [moles of total products]/[moles of Fe introduced].

The effect of some reaction variables such as reaction temperature, pH, amount of Pd/AC, and Fe content in Fe-ZSM-5 on the catalytic performance was investigated. The total product yield increased with increasing reaction temperature in the temperature range of 0–50 °C (Figure 2a, Table S3). It is worth mentioning that the concentration of hydrogen peroxide after a reaction generally decreased with increasing temperature. Therefore, it was concluded that the formation of hydrogen peroxide was favored at low temperatures while methane oxidation was favorable at high temperatures. As hydrogen peroxide formed from H₂ and O₂ was used to oxidize methane, the total product yield did not increase exponentially with reaction temperature, as observed in most chemical reactions. The selectivity to methane oxygenates decreased with increasing reaction temperature because these transformations were consecutive and methane oxygenates were more active than methane itself under the same reaction conditions. The effect of pH on catalytic performance was also investigated using 0.766 wt. % Fe-ZSM-5. The total product yield increased upon decreasing the pH from 3.3 to 0.7 (Figure 2b, Table S4). This was closely related to the fact that the final concentration of H₂O₂ after the reaction increased with decreasing pH (Table S4). The hydrogen peroxide formed from H₂ and O₂ acted as an oxidant for methane during the reaction. It has been reported that low pH is more favorable to produce H₂O₂ from H₂ and O₂ and to prevent its decomposition [38]. Finally, the effect of the amount of 1 wt. % Pd/AC and Fe content in Fe-ZSM-5 was evaluated. Since Pd/AC is responsible for H₂O₂ generation from H₂ and O₂, it is generally expected that the total yield of methane oxygenates would increase with the amount of Pd/AC. This trend was confirmed, as shown in Figure 2c (Table S5). The residual concentration of H₂O₂ appeared to decrease with the increasing amount of Pd/AC, which could be attributed to H₂O₂ decomposition over Pd metal [38]. The total product yield increased but

the selectivity to methane oxygenates decreased with Fe content in Fe-ZSM-5 (Figure 2d and Table S6). This is reasonable because the Fe species are responsible for the oxidation of methane and methane oxygenates, which are more reactive than methane under the same reaction conditions.

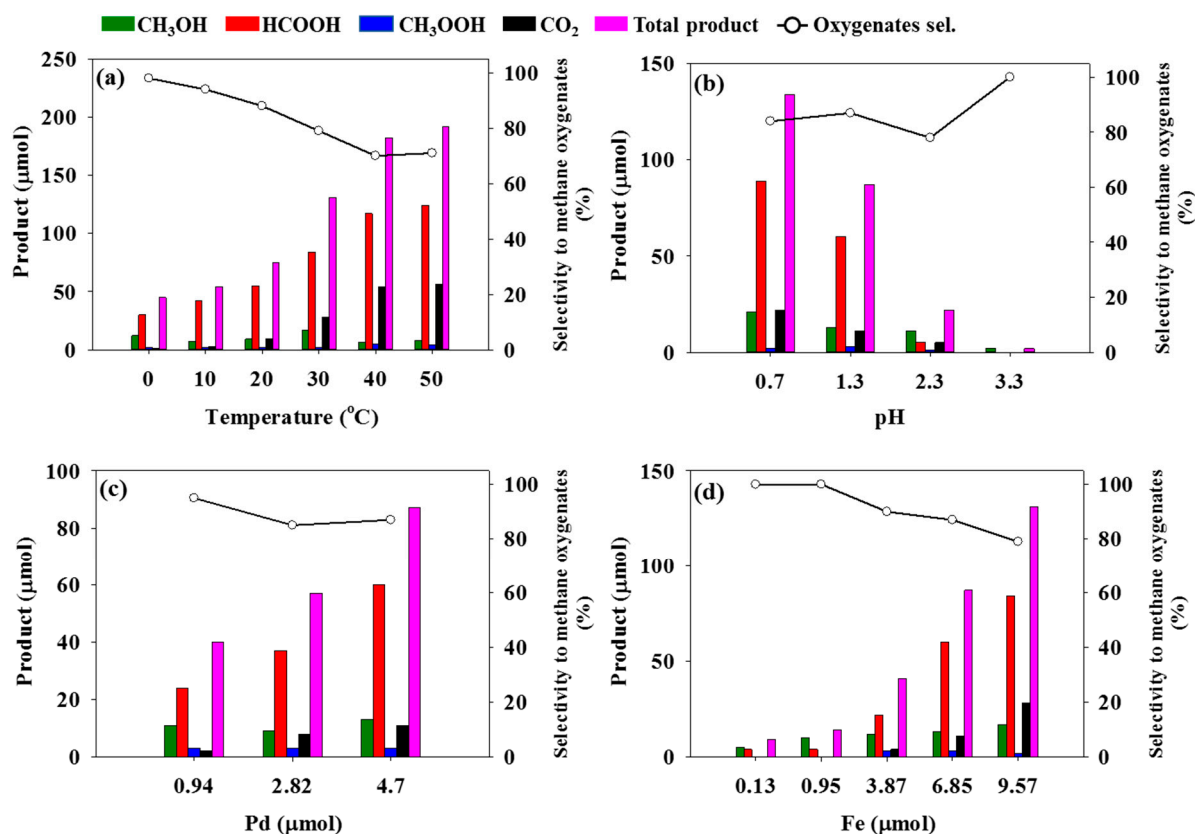


Figure 2. Performance of Fe-ZSM-5 catalysts such as 1.07 wt. % Fe-ZSM-5 (a), 0.766 wt. % Fe-ZSM-5 (b, c), and Fe-ZSM-5 with various Fe content (d) for partial oxidation of methane in the presence of H₂ and O₂ and 1 wt. % Pd/AC. Reaction conditions: 50 mg of Fe-ZSM-5 and 50 mg of 1 wt. % Pd/AC were used in all cases except for (c). Different amounts of Pd/AC were used for the case (c); reaction time = 30 min. V_{liquid} = 30 mL, V_{gas} = 90 mL, P_{CH₄} = 15 bar, P_{H₂} = 3 bar, P_{Air} = 10 bar. The reaction temperature was fixed at 30 °C in all cases except for (a). The concentration of H₂SO₄ was 15 mM in all cases except for (b).

3. Discussion

A heterogeneous catalyst is preferred over a homogeneous catalyst from a practical point of view as long as both catalysts exhibit similar catalytic performance. Based on the report [35] that a homogenous Fe catalyst was able to oxidize methane in water at low temperatures with H₂O₂ generated *in situ* from H₂ and O₂, we applied heterogeneous Fe-zeolites instead of a homogeneous Fe catalyst in this study. As this reaction is conducted in acidified water, each Fe-zeolite shows different catalytic activity and stability. Generally, a better catalytic activity implies worse catalyst stability (Table 1 and Table S2). Further study with Fe-ZSM-5 confirmed that the effect of some reaction variables such as reaction temperature, pH, and amount of catalyst was similar to that observed when the homogeneous Fe catalyst was used, as reported previously [35]. The ICP analysis of the liquid after the heterogeneous reaction conducted under different conditions supported the observation that the catalytic activity is closely related to the amount of leached Fe species. The fraction of leached metals such as Fe and Al increased slightly with increasing reaction temperature (Table S7) and concentration of sulfuric acid (Table S8). The amount of leached Fe species increased with the increasing Fe content in Fe-ZSM-5 (Table S9). However, it should be noted that the fraction of leached Fe species is independent of the Fe

content in Fe-ZSM-5 (Table S9). It is also worth mentioning that no leaching was observed from Pd/AC in all cases and only occurred when a high concentration of H_2SO_4 was used to decrease the pH to 0.7 (Table S8).

To compare the activity of homogeneous and heterogeneous catalysts for the partial oxidation of methane, this reaction was carried out using FeSO_4 and 1 wt. % Pd/AC under the same reaction conditions as those employed for the heterogeneous catalyst. Similar to the previous results [35], the total product yield increased but the selectivity to the methane oxygenates decreased with increasing concentration of FeSO_4 (Table S10). Figure 3 shows that the total product yield was proportional to the amount of homogeneous Fe species in the reaction system. This result confirmed that using the heterogeneous Fe-ZSM-5 catalyst results in total product yields that are similar to those obtained with the homogeneous catalyst whose concentration is equal to that of Fe species leached from Fe-ZSM-5. Therefore, it was concluded that the real active species for Fe-ZSM-5 catalyst in this reaction was the leached Fe species.

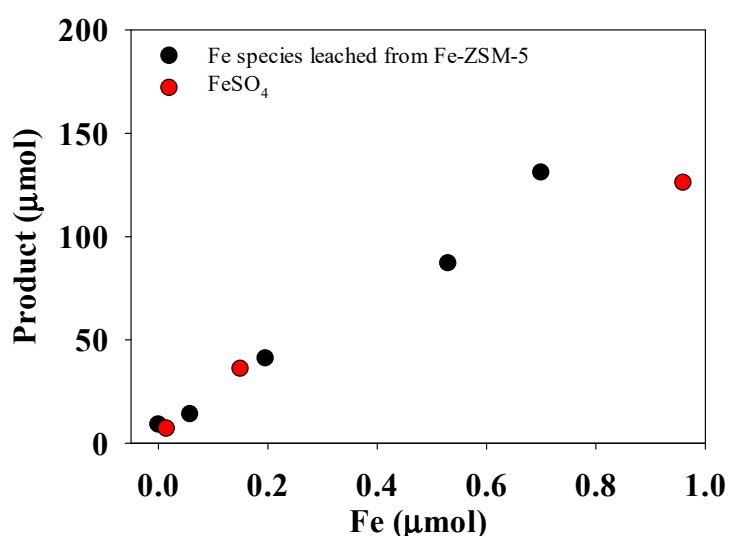


Figure 3. Total product yield as a function of the amount of Fe species in the homogeneous Fe catalyst system or in the liquid for the heterogeneous catalyst system with Fe-ZSM-5. All data were taken from Tables S6, S9 and S10.

The Fe-ZSM-5 catalyst has been reported to oxidize methane with H_2O_2 in water [25]. On the other hand, FeSO_4 itself is not active for partial oxidation of methane with H_2O_2 in water as reported in our previous work [35]. This implies that these two catalysts have different reaction mechanisms for the aqueous-phase oxidation of methane. As shown in Table S11, there was no noticeable difference in the product distribution during methane oxidation with H_2O_2 over Fe-ZSM-5 carried out under different pH. The H_2O_2 conversion was lower in the presence of H_2SO_4 than in its absence. This implies that the presence of H_2SO_4 is beneficial for the efficient utilization of H_2O_2 during methane oxidation. The contribution of leached Fe species to the oxidation of methane was examined separately. This homogeneous Fe species was confirmed to be ineffective for both methane oxidation with H_2O_2 and H_2O_2 decomposition (entry 3 in Table S11). An additional experiment was performed to compare the direct addition of H_2O_2 with *in situ* generation of H_2O_2 . The gas composition was controlled to produce 0.28 M H_2O_2 if all H_2 was completely converted into H_2O_2 . This *in situ* system (entry 4 in Table S11) provided lesser amounts of products as compared to the direct H_2O_2 addition system (entry 3 in Table S11). The addition of H_2SO_4 is necessary for the efficient generation of H_2O_2 from H_2 and O_2 but is problematic owing to the leaching problem. Note that there was no leaching in the absence of H_2SO_4 (Table S4) and only a very small amount of methanol was produced. This implies that in the case of using Fe-zeolites as catalysts, the *in situ* generation of H_2O_2 should be carried out in the absence of an acid to oxidize methane without leaching.

4. Materials and Methods

4.1. Catalyst Preparation

All Fe-zeolites were prepared via an ion-exchange method using iron(II) sulfate heptahydrate as a precursor. In this method, 2.97 g of each zeolite, such as NH₄-ZSM-5 (Zeolyst, CBV3024E, S_{BET} = 405 m²/g), NH₄-mordenite (Zeolyst, CBV21A, S_{BET} = 500 m²/g), NH₄-β (Zeolyst, CP814E, S_{BET} = 710 m²/g), NH₄-Y (Zeolyst, CBV712, S_{BET} = 730 m²/g), and NH₄-ferrierite (Zeolyst, CP914C, S_{BET} = 400 m²/g), was added into 300 mL of deionized water containing nitric acid to adjust the pH to 3. After heating the solution to 80 °C, 0.4292 g of FeSO₄·7H₂O (Sigma Aldrich, St. Louis, MO, USA) was added into the solution and stirred for 2 h. The sample was filtered, washed with deionized water, and dried in an oven at 110 °C overnight. The dried sample was calcined in static air at 550 °C for 3 h before use.

The 1 wt. % Pd/AC catalyst was prepared by a wet impregnation method using Palladium(II) chloride as a precursor. In this method, 85 mg of Pd(II)Cl₂ (Sigma Aldrich) was added into 50 mL of deionized water with a few drops of HCl solution (Samchun Pure Chemical, Pyeongtaek, Korea). Next, 4.95 g of AC (Sigma Aldrich) was added into the solution. After mixing the solution for 3 h at 60 °C, water was evaporated using a rotary evaporator. The catalyst was dried in an oven at 110 °C overnight and reduced with H₂ at 300 °C before use. The average particle size of Pd in Pd/AC was determined to be 2.5 nm based on the TEM image (Figure S2).

4.2. Catalytic Activity Test

The liquid-phase partial oxidation of methane was conducted in an autoclave with a total volume of 125 mL. The reaction temperature was maintained by two circulators (one for heating and another for cooling). A glass liner was inserted inside the autoclave to avoid the side reactions and contamination. Typically, 50 mg of Fe-zeolite and 50 mg of 1 wt. % Pd/AC, unless stated explicitly, were added into 30 mL of an aqueous solution containing sulfuric acid (Sigma Aldrich) to adjust the pH. The reactor was sealed and charged with 15 bar of methane after purging with methane five times. It was then charged with 3 bar of hydrogen and 10 bar of air. The solution was mixed vigorously at 1200 rpm with a magnetic stirrer.

4.3. Analytical Method

After the reaction, the gas-phase product was analyzed using a gas chromatograph (GC, YL instrument 6100GC) with a flame ionization detector (FID). The GC was equipped with a methanizer unit for analysis of CO₂ (or CO). The reaction solution was filtered with a membrane filter (PVDF 0.22 μm, Merck, Darmstadt, Germany) and liquid-phase products were analyzed by ¹H-NMR spectroscopy (JNM-ECZ 600R, JEOL, Tokyo, Japan). The NMR spectra were obtained at room temperature and quantified with a 0.1% trimethylsilylpropanoic acid (TMSP) sodium salt/D₂O standard (Euriso-top, Saclay, France). The amount of H₂O₂ remaining after each reaction was quantified by the titration method using Ce(SO₄)₂ and ferroin indicator.

The BET surface area of each catalyst was analyzed using the ASAP2020 (Micromeritics) surface area analyzer. The UV-Vis spectra were obtained using V-650 spectrophotometer (Jasco, Tokyo, Japan). The X-ray diffraction patterns of various Fe-zeolite catalysts were analyzed using the D/max-2200/PC (Rigaku, Tokyo, Japan) diffractometer. The metal content of the catalysts and amount of leached metal in the liquid were quantified by inductively coupled plasma-optical emission spectroscopy using OPTIMA 5300DV (PerkinElmer, Waltham, MA, USA). The TEM image of Pd/AC was obtained using Tecnai G2 F30 S-TWIN (FEI, Hillsboro, OR, USA).

5. Conclusions

To replace homogeneous Fe catalysts, Fe-zeolites were evaluated for the liquid-phase partial oxidation of methane with H₂O₂ generated *in situ* over Pd/AC from H₂ and O₂. Although Fe-Y and

Fe- β showed high catalytic activity, they suffered from a serious leaching problem. On the other hand, Fe-ZSM-5 was more stable than Fe-Y and Fe- β against leaching and exhibited relatively high catalytic activity. The catalytic activity of Fe-ZSM-5 with *in situ* generated H₂O₂ increased with increasing reaction temperature, concentration of H₂SO₄, amount of Pd/AC catalyst, and Fe content in Fe-ZSM-5. Further, ICP analysis of the liquid revealed that the catalytic activity was mainly dependent on the amount of the Fe species leached from Fe-ZSM-5. The dissolution of metals from Fe-ZSM-5 was facilitated in the presence of an acid. No leaching was observed in the absence of H₂SO₄. However, only a very amount of methanol was formed in this case because of the poor efficiency of the formation of H₂O₂, which is essential for methane oxidation over Fe-ZSM-5. The development of a heterogeneous catalyst that can produce H₂O₂ from H₂ and O₂ in the absence of an acid is key to oxidizing methane using Fe-ZSM-5 without leaching.

Supplementary Materials: The following are available online at <http://www.mdpi.com/2073-4344/10/3/299/s1>, Table S1: Metal contents and BET surface area of Fe-zeolites, Table S2: Metal contents in Fe-zeolites before the reaction and in the liquid after the reaction, Table S3: Catalytic performance of 1.07 wt. % Fe-ZSM-5 and 1 wt. % Pd/AC at different reaction temperatures in the partial oxidation of methane, Table S4: Effect of pH on the performance of 0.766 wt. % Fe-ZSM-5 and 1 wt. % Pd/AC catalysts in the partial oxidation of methane, Table S5: Effect of 1 wt. % Pd/AC on the catalytic performance of 0.766 wt. % Fe-ZSM-5 and 1 wt. % Pd/AC in the partial oxidation of methane, Table S6: Effect of Fe content in Fe-ZSM-5 on the performance of Fe-ZSM-5 and 1 wt. % Pd/AC catalysts in the partial oxidation of methane; Table S7: Metal content in the liquid and the fraction of leached metal after the reaction with 1.07 wt. % Fe-ZSM-5 and 1 wt. % Pd/AC at different temperatures, Table S8: Metal content in the liquid and the fraction of leached metal after a reaction with 0.766 wt. % Fe-ZSM-5 and 1 wt. % Pd/AC at different pH, Table S9: Metal content in the liquid and the fraction of leached metal after a reaction with Fe-ZSM-5 containing different Fe contents and 1 wt. % Pd/AC catalysts, Table S10: Catalytic performance of different concentrations of 1 wt. % Pd/AC and FeSO₄ in the partial oxidation of methane, Table S11: Catalytic performance for partial oxidation of methane under different conditions, Figure S1: XRD patterns of (a) H-ZSM-5 and Fe-ZSM-5, (b) H-mordenite and Fe-mordenite, (c) H- β and Fe- β , (d) H-Y and Fe-Y, and (e) H-ferrierite and Fe-ferrierite, Figure S2: TEM image (a) and particle size distribution of Pd metal (b) of 1 wt. % Pd/AC.

Author Contributions: J.K. and E.D.P. designed the experiments; J.K. performed and collected data; J.K. and E.D.P. analyzed the data and wrote the paper. All authors have read and agreed to the published version of the manuscript.

Funding: This work was supported by C1 Gas Refinery Program through the National Research Foundation of Korea (NRF) funded by the Ministry of Science, ICT and Future Planning (2015M3D3A1A01064899). This work was also supported by the Human Resources Program in Energy Technology (No. 20154010200820) of the Korea Institute of Energy Technology Evaluation and Planning, which is granted financial resources by the Ministry of Trade, Industry and Energy of the Republic of Korea.

Conflicts of Interest: The authors declare no conflict of interest.

References

1. McFarland, E. Unconventional Chemistry for Unconventional Natural Gas. *Science* **2012**, *338*, 340–342. [[CrossRef](#)]
2. Blanksby, S.J.; Ellison, G.B. Bond Dissociation Energies of Organic Molecules. *Acc. Chem. Res.* **2003**, *36*, 255–263. [[CrossRef](#)] [[PubMed](#)]
3. Bao, J.; Yang, G.; Yoneyama, Y.; Tsubaki, N. Significant Advances in C1 Catalysis: Highly Efficient Catalysts and Catalytic Reactions. *ACS Catal.* **2019**, *9*, 3026–3053. [[CrossRef](#)]
4. Park, M.B.; Park, E.D.; Ahn, W. Recent Progress in Direct Conversion of Methane to Methanol Over Copper-Exchanged Zeolites. *Front. Chem.* **2019**, *7*, 514. [[CrossRef](#)] [[PubMed](#)]
5. Park, M.B.; Ahn, S.H.; Mansouri, A.; Ranocchiari, M.; Bokhoven, J.A. Comparative Study of Diverse Copper Zeolites for the Conversion of Methane into Methanol. *ChemCatChem* **2017**, *9*, 3705–3713. [[CrossRef](#)]
6. Wang, X.; Martin, N.M.; Nilsson, J.; Carlson, S.; Gustafson, J.; Skoglundh, M.; Carlsson, P. Copper-Modified Zeolites and Silica for Conversion of Methane to Methanol. *Catalysts* **2018**, *8*, 545. [[CrossRef](#)]
7. Tomkins, P.; Ranocchiari, M.; Bokhoven, J.A. Direct conversion of methane to methanol under mild conditions over Cu-zeolites and beyond. *Acc. Chem. Res.* **2017**, *50*, 418–425. [[CrossRef](#)]
8. Kim, Y.; Kim, T.Y.; Lee, H.; Yi, J. Distinct activation of Cu-MOR for direct oxidation of methane to methanol. *Chem. Commun.* **2017**, *53*, 4116–4119. [[CrossRef](#)]

9. Wood, b.J.; Reimer, J.A.; Bell, A.T.; Janicke, M.T.; Ott, K.C. Methanol formation on Fe/Al-MFI via the oxidation of methane by nitrous oxide. *J. Catal.* **2004**, *225*, 300–306. [[CrossRef](#)]
10. Starokon, E.V.; Parfenov, M.V.; Arzumanov, S.S.; Pirutko, L.V.; Stepanov, A.G.; Panov, G.I. Oxidation of methane to methanol on the surface of FeZSM-5 zeolite. *J. Catal.* **2013**, *300*, 47–54. [[CrossRef](#)]
11. Sushkevich, V.L.; Palagin, D.; Ranocchiari, M.; van Bokhoven, J.A. Selective Anaerobic Oxidation of Methane Enables Direct Synthesis of Methanol. *Science* **2017**, *356*, 523–527. [[CrossRef](#)] [[PubMed](#)]
12. Lee, S.H.; Kang, J.K.; Park, E.D. Continuous methanol synthesis directly from methane and steam over Cu(II)-exchanged mordenite. *Korean J. Chem. Eng.* **2018**, *35*, 2145–2149. [[CrossRef](#)]
13. Periana, R.A.; Taube, D.J.; Gamble, S.; Taube, H.; Satoh, T.; Fujii, H. Platinum Catalysts for the High-Yield Oxidation of Methane to a Methanol Derivative. *Science* **1998**, *280*, 560–564. [[CrossRef](#)] [[PubMed](#)]
14. Soorholtz, M.; White, R.J.; Zimmermann, T.; Titirici, M.M.; Antonietti, M.; Palkovits, R.; Schüth, F. Direct methane oxidation over Pt-modified nitrogen-doped carbons. *Chem. Commun.* **2013**, *49*, 240–242. [[CrossRef](#)]
15. Zimmermann, T.; Bilke, M.; Soorholtz, M.; Schüth, F. Influence of Catalyst Concentration on Activity and Selectivity in Selective Methane Oxidation with Platinum Compounds in Sulfuric Acid and Oleum. *ACS Catal.* **2018**, *8*, 9262–9268. [[CrossRef](#)]
16. Dang, H.T.; Lee, H.W.; Lee, J.; Choo, H.; Hong, S.H.; Cheong, M.; Lee, H. Enhanced Catalytic Activity of (DMSO)₂PtCl₂ for the Methane Oxidation in the SO₃–H₂SO₄ System. *ACS Catal.* **2018**, *8*, 11854–11862. [[CrossRef](#)]
17. Periana, R.A.; Mironov, O.; Taube, D.; Bhalla, G.; Jones, C.J. Catalytic, Oxidative Condensation of CH₄ to CH₃COOH in One Step via CH Activation. *Science* **2003**, *301*, 814–818. [[CrossRef](#)]
18. An, Z.; Pan, X.; Liu, X.; Han, X.; Bao, X. Combined redox couples for catalytic oxidation of methane by dioxygen at low temperatures. *J. Am. Chem. Soc.* **2006**, *128*, 16028–16029. [[CrossRef](#)]
19. Lin, M.; Hogan, T.E.; Sen, A. Catalytic Carbon–Carbon and Carbon–Hydrogen Bond Cleavage in Lower Alkanes. Low-Temperature Hydroxylations and Hydroxycarbonylations with Dioxygen as the Oxidant. *J. Am. Chem. Soc.* **1996**, *118*, 4574–4580. [[CrossRef](#)]
20. Kwon, Y.; Kim, T.Y.; Kwon, G.; Yi, J.; Lee, H. Selective Activation of Methane on Single-Atom Catalyst of Rhodium Dispersed on Zirconia for Direct Conversion. *J. Am. Chem. Soc.* **2017**, *139*, 17694–17699. [[CrossRef](#)]
21. Yuan, Q.; Deng, W.; Zhang, Q.; Wang, Y. Osmium-catalyzed selective oxidations of methane and ethane with hydrogen peroxide in aqueous medium. *Adv. Synth. Catal.* **2007**, *349*, 1199–1209. [[CrossRef](#)]
22. Periana, R.A.; Taube, D.J.; Evitt, E.R.; Loffler, D.G.; Wentrcek, P.R.; Voss, G.; Masuda, T. A Mercury-Catalyzed, High-Yield System for the Oxidation of Methane to Methanol. *Science* **1993**, *259*, 340–343. [[CrossRef](#)] [[PubMed](#)]
23. Park, E.D.; Hwang, Y.; Lee, C.W.; Lee, J.S. Copper- and vanadium-catalyzed methane oxidation into oxygenates with *in situ* generated H₂O₂ over Pd/C. *Appl. Catal. A: General* **2003**, *247*, 269–284. [[CrossRef](#)]
24. Seki, Y.; Mizuno, N.; Misono, M. High-yield liquid-phase oxygenation of methane with hydrogen peroxide catalyzed by 12-molybdovanadophosphoric acid catalyst precursor. *Appl. Catal. A: General* **1997**, *158*, L47–L51. [[CrossRef](#)]
25. Hammond, C.; Forde, M.M.; Ab Rahim, M.H.; Thetford, A.; He, Q.; Jenkins, R.L.; Dimitratos, N.; Lopez-Sanchez, J.A.; Dummer, N.F.; Murphy, D.M.; et al. Direct catalytic conversion of methane to methanol in an aqueous medium by using copper-promoted Fe-ZSM-5. *Angew. Chem. Int. Ed.* **2012**, *51*, 5129–5133. [[CrossRef](#)]
26. Cui, X.; Li, H.; Cui, X.; Li, H.; Wang, Y.; Hu, Y.; Hua, L.; Li, H.; Han, X. Room-Temperature Methane Conversion by Graphene-Confined Single Iron Atoms Room-Temperature Methane Conversion by Graphene-Confined Single Iron Atoms. *CHEM* **2018**, *4*, 1–9. [[CrossRef](#)]
27. Yamanaka, I.; Soma, M.; Otsuka, K. Oxidation of Methane to Methanol with Oxygen Catalysed by Europium Trichloride at Room Temperature. *J. Chem. Soc. Chem. Commun.* **1995**, *21*, 2235–2236. [[CrossRef](#)]
28. Vargaftik, M.N.; Stolarov, I.P.; Moiseev, I.I. Highly Selective Partial Oxidation of Methane to Methyl Trifluoroacetate. *J. Chem. Soc. Chem. Commun.* **1990**, *15*, 1049–1050. [[CrossRef](#)]
29. Strassner, T.; Ahrens, S.; Muehlhofer, M.; Munz, D.; Zeller, A. Cobalt-Catalyzed Oxidation of Methane to Methyl Trifluoroacetate by Dioxygen. *Eur. J. Inorg. Chem.* **2013**, *21*, 3659–3663. [[CrossRef](#)]
30. Ravi, M.; van Bokhoven, J.A. Homogeneous Copper-Catalyzed Conversion of Methane to Methyl Trifluoroacetate in High Yield at Low Pressure. *ChemCatChem* **2018**, *10*, 2383–2386. [[CrossRef](#)]
31. Ab Rahim, M.H.; Armstrong, R.D.; Hammond, C.; Dimitratos, N.; Freakley, S.J.; Forde, M.M.; Morgan, D.J.; Lalev, G.; Jenkins, R.L.; Lopez-Sanchez, J.A.; et al. Low temperature selective oxidation of methane to methanol using titania supported gold palladium copper catalysts. *Catal. Sci. Technol.* **2016**, *6*, 3410–3418. [[CrossRef](#)]

32. Lewis, R.J.; Bara-Estaun, A.; Agarwal, N.; Freakley, S.J.; Morgan, D.J.; Hutchings, G.J. The Direct Synthesis of H₂O₂ and Selective Oxidation of Methane to Methanol Using HZSM-5 Supported AuPd Catalysts. *Catal. Lett.* **2019**, *149*, 3066–3075. [[CrossRef](#)]
33. He, Y.; Luan, C.; Fang, Y.; Feng, X.; Peng, X.; Yang, G.; Tsubaki, N. Low-temperature direct conversion of methane to methanol over carbon materials supported Pd-Au nanoparticles. *Catal. Today* **2020**, *339*, 48–53. [[CrossRef](#)]
34. Jin, Z.; Wang, L.; Zuidema, E.; Mondal, K.; Zhang, M.; Zhang, J.; Wang, C.; Meng, X.; Yang, H.; Mesters, C.; et al. Hydrophobic zeolite modification for *in situ* peroxide formation in methane oxidation to methanol. *Science* **2020**, *367*, 193–197. [[PubMed](#)]
35. Kang, J.; Park, E.D. Aqueous-Phase Selective Oxidation of Methane with Oxygen over Iron Salts and Pd/C in the Presence of Hydrogen. *ChemCatChem* **2019**, *11*, 4247–4251. [[CrossRef](#)]
36. Centi, G.; Perathoner, S.; Pino, F.; Arrigo, R.; Giordano, G.; Katovic, A.; Pedulà, V. Performances of Fe-[Al, B]MFI catalysts in benzene hydroxylation with N₂O: The role of zeolite defects as host sites for highly active iron species. *Catal. Today* **2005**, *110*, 211–220. [[CrossRef](#)]
37. Hammond, C.; Dimitratos, N.; Lopez-Sanchez, J.A.; Jenkins, R.L.; Whiting, G.; Kondrat, S.A.; ab Rahim, M.H.; Forde, M.M.; Thetford, A.; Hagen, H.; et al. Aqueous-Phase Methane Oxidation over Fe-MFI Zeolites; Promotion through Isomorphous Framework Substitution. *ACS Catal.* **2013**, *3*, 1835–1844. [[CrossRef](#)]
38. Choudhary, V.R.; Samanta, C. Role of chloride or bromide anions and protons for promoting the selective oxidation of H₂ by O₂ to H₂O₂ over supported Pd catalysts in an aqueous medium. *J. Catal.* **2006**, *238*, 28–38. [[CrossRef](#)]



© 2020 by the authors. Licensee MDPI, Basel, Switzerland. This article is an open access article distributed under the terms and conditions of the Creative Commons Attribution (CC BY) license (<http://creativecommons.org/licenses/by/4.0/>).